Wang et al. Nanoscale Research Letters (2017) 12:276
DOI 10.1186/s11671-017-2048-2

Nanoscale Research Letters

NANO EXPRESS Open Access

# Engineering the Complex-Valued Constitutive Parameters of Metamaterials for Perfect Absorption

Pengwei Wang[1], Naibo Chen[1], Chaojun Tang[1*], Jing Chen[2,3*], Fanxin Liu[1,3], Saiqian Sheng[1], Bo Yan[1] and Chenghua Sui[1]

**Abstract**

We theoretically studied how to directly engineer the constitutive parameters of metamaterials for perfect absorbers of electromagnetic waves. As an example, we numerically investigated the necessary refractive index $n$ and extinction coefficient $k$ and the relative permittivity $\varepsilon$ and permeability $\mu$ of a metamaterial anti-reflection layer, which could cancel the reflection from a hydrogenated amorphous silicon (α-Si:H) thin film on a metal substrate, within the visible wavelength range from 300 to 800 nm. We found that the metamaterial anti-reflection layer should have a negative refractive index ($n < 0$) for short-wavelength visible light but have a positive refractive index ($n > 0$) for long-wavelength visible light. The relative permittivity $\varepsilon$ and permeability $\mu$ could be fitted by the Lorentz model, which exhibited electric and magnetic resonances, respectively.

**Keywords:** Metamaterials, Perfect absorbers, Anti-reflection coating, Light harvesting

## Background

In recent years, metamaterial-based electromagnetic wave perfect absorbers have attracted too much interest [1–3], owing to a wide variety of potential applications such as thermal emitters [4–6], sensor [7–10], photodetection [11, 12], solar cells or thermo-photovoltaics [13–17], and so on. In 2008, Landy et al. first experimentally demonstrated metamaterial perfect absorbers in the microwave region, by matching the effective wave impedance of metamaterials to the free-space wave impedance [18]. Their designed metamaterial perfect absorbers consist of two standard split-ring resonators connected by the inductive ring parallel to the split wire and a cut wire in a parallel plane separated by a substrate. This seminal work in the microwave regime has inspired many studies on metamaterial perfect absorbers in other frequency regimes including terahertz [19–21], mid-infrared [22, 23], near-infrared [24–26], and visible realm [27–29]. At the same time, there also have been many efforts to make metamaterial perfect absorbers as efficient and effective as possible, through carefully engineering their versatile properties like polarization independence [30–33], broad incident angle [34–37], broad bandwidth or multi-band [38–41], tunability [42–44], and flexibility [45, 46]. In most metamaterial perfect absorbers, there is always a three-layer design with a ground plane or metallic substrate supporting a dielectric and top metallic nanostructure [1]. The physical mechanisms behind many metamaterial perfect absorbers are essentially the same: the top metallic structure is utilized to couple to the incident electric field, and the anti-parallel currents between the two metallic layers are used to couple to the incident magnetic field. By tuning the metamaterial geometry, one could impedance match to free space at a desired frequency range [1]. For explaining the same phenomenon of perfect absorption of electromagnetic waves, there are also other physical models based on interference theory of reflected waves [47–50], such as transmission line theory [51–54], Fabry-Pérot, or other cavity resonances [55–62].

In many studies on metamaterial perfect absorbers, tailoring the morphology of the top metallic nanostructure has been explored widely as an effective way to obtain

* Correspondence: chaojuntang@zjut.edu.cn; jchen@njupt.edu.cn
[1]Center for Optics & Optoelectronics Research, Department of Applied Physics, Zhejiang University of Technology, Hangzhou 310023, China
[2]College of Electronic Science and Engineering, Nanjing University of Posts and Telecommunications, Nanjing 210023, China
Full list of author information is available at the end of the article

desired performances [1]. However, there are only few researches on directly engineering the complex-valued constitutive parameters of an artificial metamaterial for perfect absorbers of electromagnetic waves [63, 64]. For example, Ye et al. experimentally demonstrated a metamaterial perfect absorber in which the frequency-independent dispersion regions of both permittivity and permeability are stretched to an ultrawide band from 0.5 to 2.5 GHz, and the real and imaginary parts of the complex constitutive parameters are precisely tuned to satisfy a modified model of a perfectly matched layer [63]. Long et al. deduced theoretically the critical coupling condition to achieve perfect absorption for thin-film absorbers of absorbing layer/spacer layer/substrate and identified numerically the key characteristics of the absorbing layer needed for perfect absorption at a given wavelength [64].

In this work, we will theoretically show how to directly engineer the complex-valued constitutive parameters of artificial metamaterials for perfect absorbers of electromagnetic waves. Specifically speaking, for achieving ultrawideband perfect absorption within the visible wavelength range from 300 to 800 nm, we have numerically investigated the necessary refractive index $n$ and extinction coefficient $k$, and the relative permittivity $\varepsilon$ and permeability $\mu$ of a metamaterial anti-reflection layer, coating a hydrogenated amorphous silicon (α-Si:H) thin film on a metal substrate. It is found that the metamaterial anti-reflection layer should have a negative refractive index ($n < 0$) for short-wavelength visible light, but has a positive refractive index ($n > 0$) for long-wavelength visible light. As the thickness of the metamaterial anti-reflection layer is increased, the absolute value of $n$ and $k$ will become smaller. However, they will become larger when the thickness of the α-Si:H thin film is increased. The relative permittivity $\varepsilon$ and permeability $\mu$ could be fitted by the Lorentz model, exhibiting electric and magnetic resonances, respectively.

## Methods

The perfect absorber of electromagnetic waves investigated in this work is schematically shown in Fig. 1. Light is normally incident from air onto the perfect absorber, which consists of a metamaterial anti-reflection layer, and a hydrogenated amorphous silicon (α-Si:H) layer deposited on an Ag substrate. In our numerical calculations, the refractive index $n_0$ of air is 1. The metamaterial anti-reflection layer has a complex refractive index of $n_1 + ik_1$ and a thickness of $d_1$. The α-Si:H layer has a complex refractive index of $n_2 + ik_2$ and a thickness of $d_2$. The Ag substrate has a complex refractive index of $n_3 + ik_3$. In our numerical calculations, the used refractive index $n$ and the extinction coefficient $k$ of α-Si:H and Ag are presented in Fig. 2.

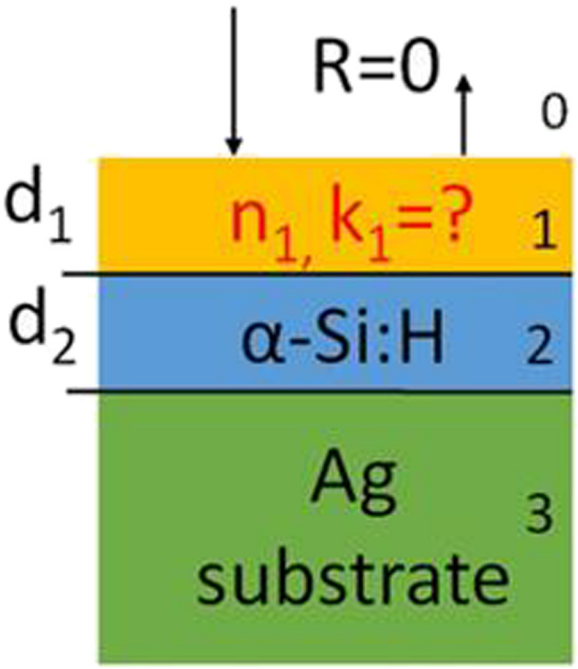


**Fig. 1** Schematic diagram of a perfect absorber of electromagnetic waves. The media labeled as 0, 1, 2, and 3 are air, metamaterial anti-reflection layer, hydrogenated amorphous silicon (α-Si:H) layer, and Ag substrate, respectively. The thicknesses of the anti-reflection and α-Si:H layers are $d_1$ and $d_2$, respectively

In the three-layer structure shown in Fig. 1, the reflection coefficient of light can be expressed as [64, 65]

$$r = \frac{r_{01} + r_{123}e^{2i\beta_1}}{1 + r_{01}r_{123}e^{2i\beta_1}}, \quad (1)$$

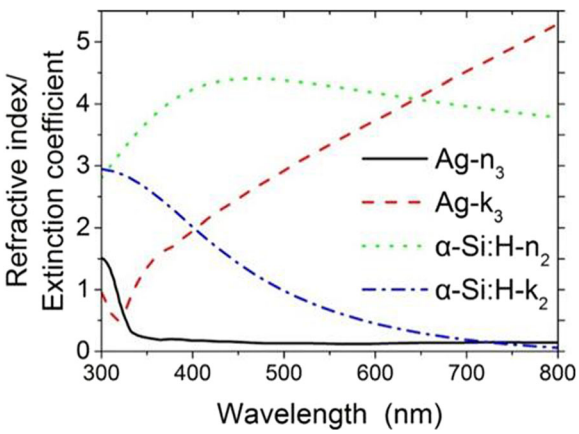


**Fig. 2** The refractive index $n$ and extinction coefficient $k$ of the Ag substrate and the hydrogenated amorphous silicon (α-Si:H) layer. The *black* (*solid*) *line* and the *red* (*dash*) *line* give the refractive index $n_1$ and extinction coefficient $k_1$ of Ag, respectively. The *green* (*dot*) *line* and the *blue* (*dash dot*) *line* give the refractive index $n_2$ and extinction coefficient $k_2$ of α-Si:H, respectively

Where $r_{123} = \frac{r_{12}+r_{23}e^{2i\beta_2}}{1+r_{12}r_{23}e^{2i\beta_2}}$, $\beta_m = \frac{2\pi}{\lambda}\tilde{n}_m d_m$, and $r_{pq} = (\tilde{n}_p - \tilde{n}_q)/(\tilde{n}_p + \tilde{n}_q)$, which denotes the Fresnel reflection coefficients from medium $p$ to medium $q$. $\tilde{n}_p = n_p + i\,k_p$ is the complex refractive index of medium $p$. $n_p$ and $k_p$ are the refractive indexes and the extinction coefficient of medium $p$. The light reflectivity is given by $R = |r|^2$. The light absorption can be written as $A = 1 - R$, because the substrate is metallic and there is no transmission.

## Results and discussion

When the reflectivity $R$ is equal to zero, the multi-layer structure shown in Fig. 1 can work as a perfect absorber. As the other physical and geometrical parameters are given, $R$ is only a function of refractive index $n_1$ and extinction coefficient $k_1$ of the anti-reflection layer. By solving numerically the equation of $R\ (n_1,\ k_1) = 0$, one can obtain the values of $n_1$ and $k_1$ [64, 66]. In Fig. 3a, b, we show the solved values of $n_1$ and $k_1$ for achieving perfect absorption in the wavelength range from 300 to 800 nm, with the thickness $d_1$ of the anti-reflection layer increased from 10 to 30 nm in steps of 2 nm, and the thickness $d_2$ of the α-Si:H layer fixed to be 15 nm. It is clearly seen in Fig. 3a that the anti-reflection layer needs a kind of material having a negative refractive index ($n_1 < 0$) for short wavelengths smaller than about 550 nm. However, the anti-reflection layer needs another kind of material having a positive refractive index ($n_1 > 0$) for longer wavelengths. As the thickness $d_1$ is increased, the absolute value of $n_1$ will become smaller, and the value of $k_1$ will also become smaller, as exhibited in Fig. 3b. We have also investigated the effect of thickness $d_2$ on the necessary refractive index $n_1$ and extinction coefficient $k_1$ for achieving perfect absorption. As clearly seen in Fig. 3c, d, both the absolute value of $n_1$ and the value of $k_1$ will become larger with increasing thickness $d_2$, which is in contrast to the case in Fig. 3a, b.

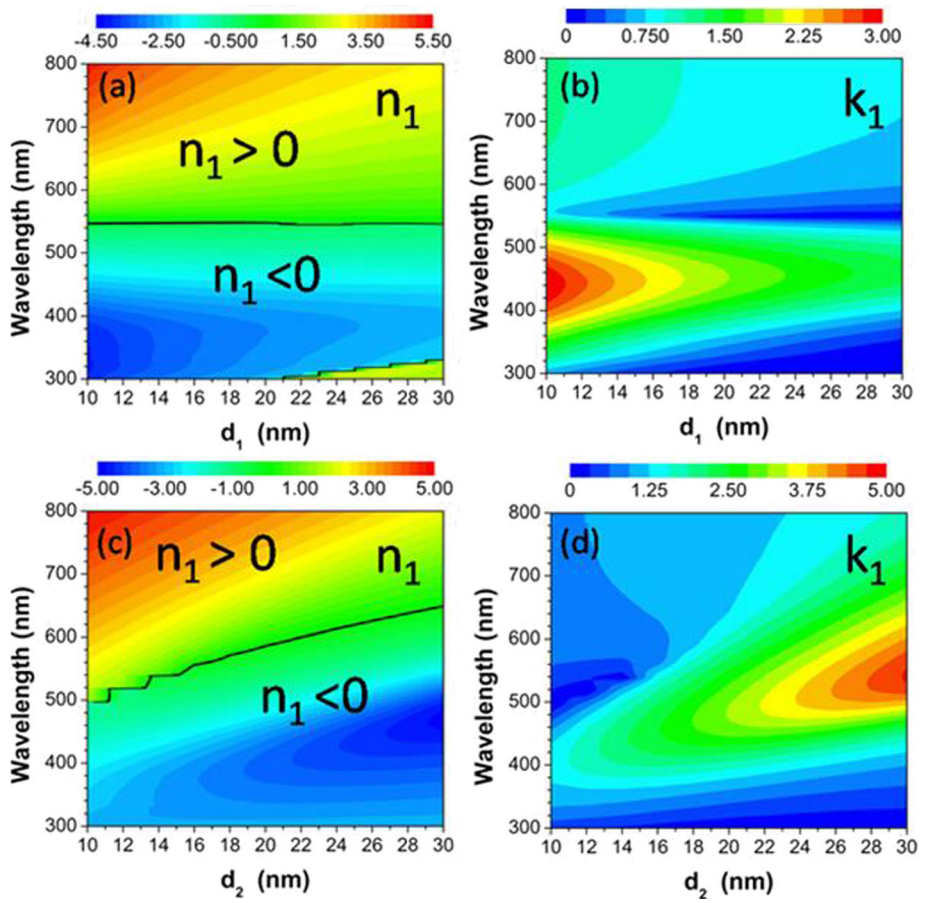


**Fig. 3** **a** The necessary refractive index $n_1$ and **b** extinction coefficient $k_1$ of the anti-reflection layer as a function of light wavelength and thickness $d_1$ for achieving perfect absorption. The wavelength is varied from 300 to 800 nm. The thickness $d_1$ of the anti-reflection layer is increased from 10 to 30 nm in steps of 2 nm. The thickness of the α-Si:H layer $d_2 = 15$ nm. **c, d** The same as with **a** and **b**, but for thickness $d_2$ increased from 10 to 30 nm, and $d_1 = 15$ nm. The *black lines* in **a** and **c** indicate the boundaries at which the refractive index $n_1$ is equal to zero

Here, we discuss the physical mechanism that underlined the perfect absorber of light waves. In order to obtain perfect absorption or zero reflection, the two terms ($r_{01}$ and $r_{123}e^{2i\beta_1}$) in Eq. (1) should have the same amplitude but opposite phase, from which one can deduce two equations to define the condition for perfect absorption [64]: $4\pi k_1 d_1/\lambda = In(R_{123}/R_{01}), 4\pi n_1 d_1/\lambda = \pi + \varphi_{01} - \varphi_{123}$, where $R_{01}$ ($R_{123}$) and $\varphi_{01}(\varphi_{123})$ denote the amplitude and the phase of $r_{01}$ ($r_{123}$), respectively. When both equations are satisfied, completely destructive interference will happen. As a result, reflection is reduced to zero, and perfect absorption is achieved.

In many cases, the permittivity and permeability are also often used to exhibit the constitutive parameters of electromagnetic materials. So, in order to further understand the conditions of perfect absorption, the relative permittivity $\varepsilon$ and permeability $\mu$ of the metamaterial anti-reflection layer are also investigated. We can calculate numerically the real and imaginary parts ($\varepsilon_r$, $\varepsilon_i$, $\mu_r$, $\mu_i$) of $\varepsilon$ and $\mu$, using the following relation of constitutive parameters in Eq. (2)

$$\begin{aligned} n &= n_1 + ik_1 \\ n &= \pm\sqrt{\varepsilon\mu} \\ \varepsilon &= \varepsilon_r + i\varepsilon_i \\ \mu &= \mu_r + i\mu_i \end{aligned} \tag{2}$$

The choice of sign "±" in Eq. (2) must ensure that $k_1$ is positive because electromagnetic waves propagating in a passive medium always suffer a loss. As an example, the dashed lines in Fig. 4 present the calculated values of the real and imaginary parts of $\varepsilon$ and $\mu$, for the thickness of the anti-reflection layer $d_1 = 15$ nm and the thickness of the α-Si:H layer $d_2 = 30$ nm. The numerical results can be fitted approximately through the Lorentz model, in which the complex permittivity and permeability can be represented as

$$\begin{aligned} \varepsilon' &= \varepsilon_1 + \frac{\omega_p^2}{{\omega_{a1}}^2 - \omega^2 - i\omega_{c1}\omega} \\ \mu' &= \mu_1 + \frac{\omega_p^2}{{\omega_{a2}}^2 - \omega^2 - i\omega_{c2}\omega} \end{aligned} \tag{3}$$

Here, $i$ is the imaginary unit, $\omega_p$ is the plasma frequency, $\omega_{a1}$, $\omega_{a2}$ are the center frequencies of the oscillators, $\omega_{c1}$, $\omega_{c2}$ are the damping frequencies, and $\varepsilon_1, \mu_1$ are the static permittivity and permeability at infinite frequency, respectively. The solid lines in Fig. 4 show the fitted results by Eq. (3), with the corresponding parameters $\varepsilon_1 = -3.9$, $\mu_1 = -1.5$, $\omega_p = 4.6 * 10^{15} Hz$, $\omega_{a1} = 3.32 * 10^{15} Hz$, $\omega_{a2} = 3.62 * 10^{15} Hz$, $\omega_{c1} = 1.3 * 10^{15} Hz$, $\omega_{c2} = 1.26 * 10^{15} Hz$. It is clearly seen in Fig. 4 that the metamaterial anti-reflection layer should have both electric and magnetic resonances.

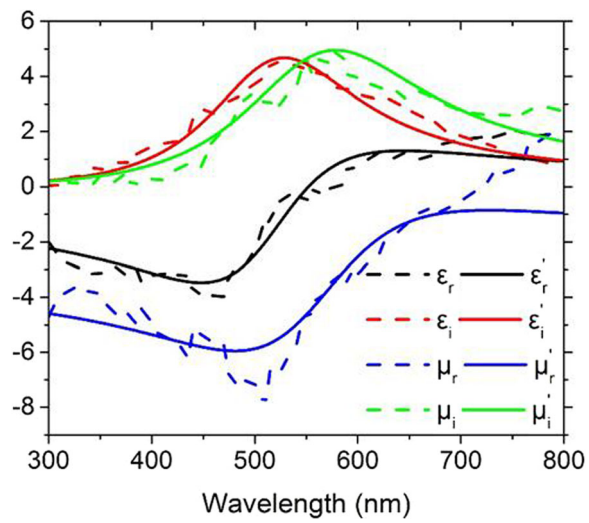


**Fig. 4** The relative permittivity $\varepsilon$ and permeability $\mu$ of the metamaterial anti-reflection layer for achieving perfect absorption, with the thickness of the anti-reflection layer $d_1 = 15$ nm and the thickness of the α-Si:H layer $d_2 = 30$ nm. The *dashed lines* give the numerically calculated values of the real and imaginary parts ($\varepsilon_r$, $\varepsilon_i$, $\mu_r$, $\mu_i$) of $\varepsilon$ and $\mu$, and the *solid lines* give the corresponding results ($\varepsilon_r$, $\varepsilon_i$, $\mu_r$, $\mu_i$) fitted through the Lorentz model

Finally, we would like to discuss the possibility of realizing the designed perfect absorber of visible light. For the perfect absorber, the complex permittivity and permeability of the anti-reflection layer must exhibit electric and magnetic resonances, respectively, which are described by the Lorentz model. When the real parts of the complex permittivity and permeability are simultaneously negative, the refractive index of the anti-reflection layer will have a negative value; otherwise, it will have a positive value. It is well-known that artificial metamaterials can exhibit Lorentz dispersion, whose constitutive parameter (either the permittivity or the permeability) obeys the *K-K* relations. In fact, with the fast development of nanofabrication technology, metamaterials with both electric and magnetic resonances have been fabricated successfully to realize negative refractive index at optical frequencies, which are composed of pairs of parallel metallic nanorods [67, 68]. Recently, an experimental work demonstrated that the real and imaginary parts of the complex constitutive parameters of metamaterials consisting of metallic split-ring resonator and rod could be deliberately controlled to produce a wide-band perfect absorption in gigahertz [63]. Based on the advancement of optical lumped nanocircuits, this approach may be extended to infrared and optical bands, as mentioned in the experimental work.

## Conclusions

In this work, we have theoretically shown how to directly engineer the complex-valued constitutive parameters of artificial metamaterials for perfect absorbers of electromagnetic waves. Specifically speaking, for achieving ultra-

wideband perfect absorption within the visible wavelength range from 300 to 800 nm, we numerically investigated the necessary refractive index $n$ and extinction coefficient $k$, and the relative permittivity $\varepsilon$ and permeability $\mu$ of a metamaterial anti-reflection layer, coating a hydrogenated amorphous silicon (α-Si:H) thin film on a metal substrate. The numerical results show that the metamaterial anti-reflection layer has a negative refractive index ($n < 0$) for short-wavelength visible light, but has a positive refractive index ($n > 0$) for long-wavelength visible light. As the thickness of the metamaterial anti-reflection layer is increased, the absolute value of $n$ and $k$ will become smaller. However, they will become larger when the thickness of the α-Si:H thin film is increased. It is also found that such a metamaterial anti-reflection layer should have both electric and magnetic resonances, and its permittivity $\varepsilon$ and permeability $\mu$ can be approximately fitted by the Lorentz model. We hope that these results presented in this work could provide another approach to design perfect absorbers of electromagnetic waves, with the fast development of nanofabrication technology in metamaterials.

#### Acknowledgements
This work is financially supported by the State Key Program for Basic Research of China (SKPBRC) under Grant Nos. 2013CB632703 and 2012CB921501, the National Natural Science Foundation of China (NSFC) under Grant Nos.11574270, 11304159, 11104136, 91221206, and 51271092, the Natural Science Foundation of Zhejiang Province under Grant Nos. LY14A040004 and LY15A040005, the Natural Science Foundation of Jiangsu Province Grant No. BK20161512, the Qing Lan Project of Jiangsu Province, the Specialized Research Fund for the Doctoral Program of Higher Education of China under Grant No. 20133223120006, and the NUPTSF under Grant No. NY217045.

#### Authors' Contributions
PW and NC contributed equally to this work. PW, NC, CT, and JC did the calculations. CT and JC wrote the manuscript. All authors read and approved the final manuscript.

#### Competing Interests
The authors declare that they have no competing interests.

## Publisher's Note


#### Author details
[1]Center for Optics & Optoelectronics Research, Department of Applied Physics, Zhejiang University of Technology, Hangzhou 310023, China. [2]College of Electronic Science and Engineering, Nanjing University of Posts and Telecommunications, Nanjing 210023, China. [3]National Laboratory of Solid State Microstructures, Nanjing University, Nanjing 210093, China.

Received: 9 February 2017 Accepted: 5 April 2017
Published online: 17 April 2017

#### References
1. Watts CM, Liu XL, Padilla WJ (2012) Metamaterial electromagnetic wave absorbers. Adv Mater 24:OP98–OP120
2. Cui YX, He YR, Jin Y, Ding F, Yang L, Ye YQ, Zhong SM, Lin YY, He SL (2014) Plasmonic and metamaterial structures as electromagnetic absorbers. Laser Photonics Rev 8:495–520
3. Ra'di Y, Simovski CR, Tretyakov SA (2015) Thin perfect absorbers for electromagnetic waves: theory, design, and realizations. Phys Rev Appl 3:037001
4. Diem M, Koschny T, Soukoulis CM (2009) Wide-angle perfect absorber/thermal emitter in the terahertz regime. Phys Rev B 79:033101
5. Liu XL, Tyler T, Starr T, Starr AF, Jokerst NM, Padilla WJ (2011) Taming the blackbody with infrared metamaterials as selective thermal emitters. Phys Rev Lett 107:045901
6. Argyropoulos C, Le KQ, Mattiucci N, D'Aguanno G, Alu A (2013) Broadband absorbers and selective emitters based on plasmonic Brewster metasurfaces. Phys Rev B 87:205112
7. Liu N, Mesch M, Weiss T, Hentschel M, Giessen H (2010) Infrared perfect absorber and its application as plasmonic sensor. Nano Lett 10:2342–2348
8. Tittl A, Mai P, Taubert R, Dregely D, Liu N, Giessen H (2011) Palladium-based plasmonic perfect absorber in the visible wavelength range and its application to hydrogen sensing. Nano Lett 11:4366–4369
9. Liu ZQ, Liu GQ, Huang S, Liu XS, Pan PP, Wang Y, Gu G (2015) Multispectral spatial and frequency selective sensing with ultra-compact cross-shaped antenna plasmonic crystals. Sens Actuator B Chem 215:480–488
10. Liu ZQ, Liu GQ, Fu GL, Liu XS, Huang ZP, Gu G (2016) All-metal metasurfaces for narrowband light absorption and high performance sensing. J Phys D Appl Phys 49:445104
11. Li W, Valentine J (2014) Metamaterial perfect absorber based hot electron photodetection. Nano Lett 14:3510–3514
12. Yu P, Wu J, Ashalley E, Govorov A, Wang ZM (2016) Dual-band absorber for multispectral plasmon-enhanced infrared photodetection. J Phys D Appl Phys 49:365101
13. Wang Y, Sun T, Paudel T, Zhang Y, Ren Z, Kempa K (2012) Metamaterial-plasmonic absorber structure for high efficiency amorphous silicon solar cells. Nano Lett 12:440–445
14. Tang MY, Zhou L, Gu S, Zhu WD, Wang Y, Xu J, Deng ZT, Yu T, Lu ZD, Zhu J (2016) Fine-tuning the metallic core-shell nanostructures for plasmonic perovskite solar cells. Appl Phys Lett 109:183901
15. Wu CH, Neuner B, John J, Milder A, Zollars B, Savoy S, Shvets G (2012) Metamaterial-based integrated plasmonic absorber/emitter for solar thermo-photovoltaic systems. J Optics 14:024005
16. Vora A, Gwamuri J, Pala N, Kulkarni A, Pearce JM, Guney DO (2014) Exchanging Ohmic losses in metamaterial absorbers with useful optical absorption for photovoltaics. Sci Rep 4:4901
17. Tang CJ, Yan ZD, Wang QG, Chen J, Zhu MW, Liu B, Liu FX, Sui CH (2015) Ultrathin amorphous silicon thin-film solar cells by magnetic plasmonic metamaterial absorbers. RSC Adv 5:81866–81874
18. Landy NI, Sajuyigbe S, Mock JJ, Smith DR, Padilla WJ (2008) Perfect metamaterial absorber. Phys Rev Lett 100:207402
19. Tao H, Landy NI, Bingham CM, Zhang X, Averitt RD, Padilla WJ (2008) A metamaterial absorber for the terahertz regime: design, fabrication and characterization. Opt Express 16:7181–7188
20. Wen QY, Zhang HW, Xie YS, Yang QH, Liu YL (2009) Dual band terahertz metamaterial absorber: design, fabrication, and characterization. Appl Phys Lett 95:241111
21. Shchegolkov DY, Azad AK, O'Hara JF, Simakov EI (2010) Perfect subwavelength fishnetlike metamaterial-based film terahertz absorbers. Phys Rev B 82:205117
22. Liu XL, Starr T, Starr AF, Padilla WJ (2010) Infrared spatial and frequency selective metamaterial with near-unity absorbance. Phys Rev Lett 104:207403
23. Jiang ZH, Yun S, Toor F, Werner DH, Mayer TS (2011) Conformal dual-band near-perfectly absorbing mid-infrared metamaterial coating. ACS Nano 5:4641–4647
24. Avitzour Y, Urzhumov YA, Shvets G (2009) Wide-angle infrared absorber based on a negative-index plasmonic metamaterial. Phys Rev B 79:045131
25. Hao JM, Wang J, Liu XL, Padilla WJ, Zhou L, Qiu M (2010) High performance optical absorber based on a plasmonic metamaterial. Appl Phys Lett 96:251104
26. Zhang BX, Zhao YH, Hao QZ, Kiraly B, Khoo IC, Chen SF, Huang TJ (2011) Polarization-independent dual-band infrared perfect absorber based on a metal-dielectric-metal elliptical nanodisk array. Opt Express 19:15221–15228
27. Aydin K, Ferry VE, Briggs RM, Atwater HA (2011) Broadband polarization-independent resonant light absorption using ultrathin plasmonic super absorbers. Nat Comm 2:517
28. Hao JM, Zhou L, Qiu M (2011) Nearly total absorption of light and heat generation by plasmonic metamaterials. Phys Rev B 83:165107
29. Hedayati MK, Javaherirahim M, Mozooni B, Abdelaziz R, Tavassolizadeh A, Chakravadhanula ASK, Zaporojtchenko V, Strunkus T, Faupel F, Elbahri M

(2011) Design of a perfect black absorber at visible frequencies using plasmonic metamaterials. Adv Mater 23:5410–5414
30. Landy NI, Bingham CM, Tyler T, Jokerst N, Smith DR, Padilla WJ (2009) Design, theory, and measurement of a polarization-insensitive absorber for terahertz imaging. Phys Rev B 79:125104
31. Grant J, Ma Y, Saha S, Khalid A, Cumming DRS (2011) Polarization insensitive, broadband terahertz metamaterial absorber. Opt Lett 36:3476–3478
32. Huang L, Chen H (2011) Multi-band and polarization insensitive metamaterial absorber. Prog Electromagn Res 113:103–110
33. Huang L, Chowdhury DR, Ramani S, Reiten MT, Luo SN, Taylor AJ, Chen HT (2012) Experimental demonstration of terahertz metamaterial absorbers with a broad and flat high absorption band. Opt Lett 37:154–156
34. Cheng Q, Cui TJ, Jiang WX, Cai BG (2010) An omnidirectional electromagnetic absorber made of metamaterials. New J Phys 12:063006
35. Wu CH, Neuner B, Shvets G, John J, Milder A, Zollars B, Savoy S (2011) Large-area wide-angle spectrally selective plasmonic absorber. Phys Rev B 84:075102
36. Li L, Yang Y, Liang CH (2011) A wide-angle polarization-insensitive ultra-thin metamaterial absorber with three resonant modes. J Appl Phys 110:063702
37. Shen XP, Cui TJ, Zhao JM, Ma HF, Jiang WX, Li H (2011) Polarization-independent wide-angle triple-band metamaterial absorber. Opt Express 19: 9401–9407
38. Narimanov EE, Kildishev AV (2009) Optical black hole: broadband omnidirectional light absorber. Appl Phys Lett 95:041106
39. Wu D, Liu YM, Li RF, Chen L, Ma R, Liu C, Ye H (2016) Infrared perfect ultra-narrow band absorber as plasmonic sensor. Nanoscale Res Lett 11:483
40. Cui YX, Fung KH, Xu J, Ma HJ, Jin Y, He SL, Fang NX (2012) Ultrabroadband light absorption by a sawtooth anisotropic metamaterial slab. Nano Lett 12: 1443–1447
41. Chen K, Adato R, Altug H (2012) Dual-band perfect absorber for multispectral plasmon-enhanced infrared spectroscopy. ACS Nano 6:7998–8006
42. Zhu B, Feng YJ, Zhao JM, Huang C, Jiang T (2010) Switchable metamaterial reflector/absorber for different polarized electromagnetic waves. Appl Phys Lett 97:051906
43. Kats MA, Sharma D, Lin J, Genevet P, Blanchard R, Yang Z, Qazilbash MM, Basov DN, Ramanathan S, Capasso F (2012) Ultra-thin perfect absorber employing a tunable phase change material. Appl Phys Lett 101:221101
44. Bermel P, Ghebrebrhan M, Harradon M, Yeng YX, Celanovic I, Joannopoulos JD, Soljacic M (2011) Tailoring photonic metamaterial resonances for thermal radiation. Nanoscale Res Lett 6:549
45. Tao H, Bingham CM, Strikwerda AC, Pilon D, Shrekenhamer D, Landy NI, Fan K, Zhang X, Padilla WJ, Averitt RD (2008) Highly flexible wide angle of incidence terahertz metamaterial absorber: design, fabrication, and characterization. Phys Rev B 78:241103
46. Singh PK, Korolev KA, Afsar MN, Sonkusale S (2011) Single and dual band 77/95/110 GHz metamaterial absorbers on flexible polyimide substrate. Appl Phys Lett 99:264101
47. Chen HT, Zhou JF, O'Hara JF, Chen F, Azad AK, Taylor AJ (2010) Antireflection coating using metamaterials and identification of its mechanism. Phys Rev Lett 105:073901
48. Chen HT (2012) Interference theory of metamaterial perfect absorbers. Opt Express 20:7165–7172
49. Shen XP, Yang Y, Zang YZ, Gu JQ, Han JG, Zhang WL, Cui TJ (2012) Triple-band terahertz metamaterial absorber: design, experiment, and physical interpretation. Appl Phys Lett 101:154102
50. Sun JB, Liu LY, Dong GY, Zhou J (2011) An extremely broad band metamaterial absorber based on destructive interference. Opt Express 19: 21155–21162
51. Wen QY, Xie YS, Zhang HW, Yang QH, Li YX, Liu YL (2009) Transmission line model and fields analysis of metamaterial absorber in the terahertz band. Opt Express 17:20256–20265
52. Pang YQ, Cheng HF, Zhou YJ, Wang J (2013) Analysis and design of wire-based metamaterial absorbers using equivalent circuit approach. J Appl Phys 113:114902
53. Hokmabadi MP, Wilbert DS, Kung P, Kim SM (2013) Design and analysis of perfect terahertz metamaterial absorber by a novel dynamic circuit model. Opt Express 21:16455–16465
54. Costa F, Genovesi S, Monorchio A, Manara G (2013) A circuit-based model for the interpretation of perfect metamaterial absorbers. IEEE Trans Antennas Propag 61:1201–1209
55. Peng XY, Wang B, Lai S, Zhang DH, Teng JH (2012) Ultrathin multi-band planar metamaterial absorber based on standing wave resonances. Opt Express 20:27756–27765
56. Zheng HY, Jin XR, Park JW, Lu YH, Rhee JY, Jang WH, Cheong H, Lee YP (2012) Tunable dual-band perfect absorbers based on extraordinary optical transmission and Fabry-Perot cavity resonance. Opt Express 20:24002-24009
57. Alaee R, Farhat M, Rockstuhl C, Lederer F (2012) A perfect absorber made of a graphene micro-ribbon metamaterial. Opt Express 20:28017–28024
58. Zhu SW, Li Z, Li YY (2013) Triple-layer Fabry-Perot absorber with near-perfect absorption in visible and near-infrared regime. Opt Express 21: 25307–25315
59. Chau YFC, Chao CTC, Rao JY, Chiang HP, Lim CM, Lim RC, Voo NY (2016) Tunable optical performances on a periodic array of plasmonic bowtie nanoantennas with hollow cavities. Nanoscale Res Lett 11:411
60. Liu ZQ, Liu GQ, Fu GL, Liu XS, Wang Y (2016) Multi-band light perfect absorption by a metal layer-coupled dielectric metamaterial. Opt Express 24: 5020–5025
61. Liu ZQ, Liu GQ, Liu XS, Huang S, Wang Y, Pan PP, Liu ML (2015) Achieving an ultra-narrow multiband light absorption meta-surface via coupling with an optical cavity. Nanotechnology 26:235702
62. Zhou L, Tan YL, Ji DX, Zhu B, Zhang P, Xu J, Gan QQ, Yu ZF, Zhu J (2016) Self-assembly of highly efficient, broadband plasmonic absorbers for solar steam generation. Sci Adv 2:e1501227
63. Ye DX, Wang ZY, Xu KW, Li H, Huangfu JT, Wang Z, Ran LX (2013) Ultrawideband dispersion control of a metamaterial surface. Phys Rev Lett 111:187402
64. Long YB, Su RM, Wang QW, Shen L, Li BW, Zheng WH (2014) Deducing critical coupling condition to achieve perfect absorption for thin-film absorbers and identifying key characteristics of absorbing materials needed for perfect absorption. Appl Phys Lett 104:091109
65. Kats MA, Blanchard R, Genevet P, Capasso F (2012) Nanometre optical coatings based on strong interference effects in highly absorbing media. Nat Mater 12:20–24
66. Huber SP, van de Kruijs RWE, Yakshin AE, Zoethout E, Boller KJ, Bijkerk F (2014) Subwavelength single layer absorption resonance antireflection coatings. Opt Express 22:490–497
67. Dolling G, Enkrich C, Wegener M, Zhou JF, Soukoulis CM, Linden S (2005) Cut-wire pairs and plate pairs as magnetic atoms for optical metamaterials. Opt Lett 30:3198–3200
68. Shalaev VM, Cai W, Chettiar UK, Yuan HK, Sarychev AK, Drachev VP, Kildishev AV (2005) Negative index of refraction in optical metamaterials. Opt Lett 30: 3356–3358